Applications of High-Temperature-Superconducting Filters and Cryo-Electronics for Satellite Communication

Edward R. Soares, *Member, IEEE*, Jeffery D. Fuller, *Member, IEEE*, Phil J. Marozick, and Robby L. Alvarez

***Abstract*—Filtering of the signals from satellites in ground-based satellite-communication receivers using high-temperature superconducting filters will be discussed in this paper, including the use of cryogenically cooled low-noise amplifiers and cooled RF switches. In addition to the RF circuits, a detailed discussion of the needed support, such as cryocoolers and Dewar, will be held. Uses for the system will be discussed and a demonstration described.**

***Index Terms*—Bandpass filters, Chebyshev filters, cryogenic electronics, microstrip, microwave amplifiers, microwave switches, satellite communication, superconducting filters, switched filters.**

I. Introduction

THE high density of satellites in geo-stationary orbits (GEO's) has increased the need for both spatial and spectral filtering. This filtering serves many purposes. First, spatial filtering is used by the antenna to reduce the interference both from other GEO satellites and terrestrial origins. Also, by using multiple very narrow high-temperature-superconducting (HTS) front-end filters, a frequency agile system can be created with very little added noise compared to a nonfiltered system. This spectral filtering is used to protect the amplifier from large out-of-band signals that could send the amplifier into compression, and also to protect the band of interest from spurious signals generated by the mixing of these signals.

Spatial filtering is provided through the antenna radiation pattern, to achieve isolation from the signals that are at the same frequency from nearby GEO satellites using the same polarization as the signal of interest. This is important because the GEO satellites use the same frequency band. The signals from U.S. C-band satellites are linearly polarized so that adjacent satellites utilize orthogonal polarization, but next nearest neighbors have the same polarization. Conventionally, spatial filtering is achieved using a large diameter dish to provide a narrow beam width with low sidelobes. However, using two or more antennas, it is possible to design the antenna radiation pattern to have nulls in the direction of the next nearest satellites (i.e., those that have the same polarization). An angular spacing of approximately 2.4° separates all the GEO satellites, thus, the next GEO satellite with the same polarization has an angular spacing of 4.8°. For example, this innovation can allow two 1-m dishes used together to have the equivalent performance of a 2.4-m dish, but with a savings of 2.95 m^2, thus vastly improving portability. These antennas are designed by SRI International (SRI), Menlo Park, CA, who have built antenna arrays for many different applications.

Due to the complementary nature of SRI's antenna's, spatial filtering, and the spectral filtering of Superconductor Technologies Inc. (STI), Santa Barbara, CA, the two companies jointly performed a demonstration at the Defense Advanced Research Projects Agency (DARPA) Headquarters, Arlington, VA. There were two main technical goals for the demonstration. One was to show that SRI's antenna array with STI's cryogenic low-noise amplifier (LNA) has superior performance to a larger antenna. The other was to show the antijam capabilities STI's switching filters bring to a satellite communication (SATCOM) system.

This paper focuses on spectral filtering and the advantages it has for interference rejection and jamming resistance. The system improvement gained with the addition of a cryogenic LNA will also be discussed. In addition, the support components needed to operate an HTS system will be discussed. The method used by STI for producing frequency-agile HTS filter front ends will also be examined.

II. Description

In SATCOM applications, the power of the received signal is very low. In conventional systems, the first element after the antenna is usually an LNA. The disadvantage of this is that the amplifier is a broad-band device, and thus, will process all the signals delivered to it, including those in the sidelobes of the antenna. This could be a problem if there are large out-of-band signals present. These large signals could saturate the amplifier. Even if the signals are not strong enough to send the amplifier into compression, these large signals could produce intermodulation products in the band of interest. If one were to place a narrow filter in front of the LNA, then the interference can be greatly attenuated and only the desired in-band signals presented to the LNA. This would improve the selectivity of the system. This is not usually done because the added loss of a conventional filter can seriously degrade the receiver sensitivity, but due to the low loss of HTS materials, this approach becomes feasible.

III. HTS Material

Passive microwave filters are fabricated from thin-film HTS materials using patterning techniques similar to those used in

Manuscript received February 22, 2000. This work was supported by the Wright-Paterson Air Force Base under Contract F33615-96-C-1929.

The authors are with Superconductor Technologies Inc., Santa Barbara CA 93111 USA.

Publisher Item Identifier S 0018-9480(00)05541-1.

the semiconductor industry. Either $YBa_2Cu_3O_{7-d}$ (YBCO) or $Tl_2BaCa_2Cu2O_8$ (TBCCO) materials may be utilized. YBCO films are deposited *in-situ* by laser ablation on both sides of either 2-in magnesium oxide (MgO) or lanthanum aluminate ($LaAlO_3$) substrates. Amorphous TBCCO precursor material is deposited on each side of an MgO substrate by laser ablation. Epitaxial thin films are then formed during a post-deposition annealing process. MgO and $LaAlO_3$ substrates are chosen for their close matching characteristics in terms of crystalline lattice and thermal coefficient of expansion with respect to oxide superconductors. They also possess desirable dielectric constants and low-loss tangents.

The unloaded quality factor (Q_u, which is a measure of the total loss of the circuit) for a resonator has three contributions

$$1/Q_u = 1/Q_{\text{subst}} + 1/Q_{\text{cond}} + 1/Q_{\text{pack}}$$

where Q_{subst} is the substrate Q, Q_{cond} is the conductor Q, and Q_{pack} is the package Q. As an example, if each of the three contributing Q's were 100 000, then the combined Q would be ~30 000, i.e., in the range where the resonator Q's described herein are observed. The only techniques providing the requisite sensitivity to measure microwave loss tangent in HTS substrates have inherent limitations. They are difficult to implement, and they cannot make measurements on small samples that would permit profiling of wafers and ingots. Measurements to date, however, suggest that substrate Qs in HTS resonators at microwave frequencies at 77 K are in the range of 100 000. Given the variability and uncertainty in this number, we are able to conclude that loss tangent is definitely a potential important limiting factor in today's resonator Q's. We must precisely determine current substrate Qs at the relevant frequency and to eliminate this uncertainty and to allow improvements in today's substrates in order to increase resonator Q's.

The microwave losses in HTS films have been studied extensively over the past ten years. The available techniques to measure surface resistance offer great precision, but have similar limitations to the current techniques available to measure loss tangent of substrates. Average R_s is measured over relatively large samples (~1 cm^2). Frequencies are limited to ~10 GHz and above, and only the top surface of the HTS film is measured, i.e., the surface next to the substrate (which might have different microwave properties) is not measured. However, using the measured value of R_s from these methods, we would expect conductor $Q > 150\,000$ in thin-film resonators at 2 GHz and 77 K [1].

As stated earlier, the HTS filters operate at a temperature of about 77 K. Due to this, they must be packaged in Dewars (i.e. thermally insulated containers) and cooled. STI builds entire systems, such as the one shown in Fig. 1. In STI's systems, an active cryocooler is used to cool the components in the Dewar.

IV. Coolers

The cryocooler is a Stirling cycle cooler with a design MTTF in excess of 50 000 h. The availability of a low-cost highly reliable compact cooling technology is critical to the successful commercialization of STI's HTS products. Since such a cryogenic cooler was not available commercially, STI developed a low-cost low-power cooler designed to cool to 77 K with sufficient heat lift for its HTS applications and with a target life of over 50 000 h. STI has developed a cooler that is both compact and reliable enough to meet industry standards and that will also exhibit significantly less unit cost in volume production. Fig. 2 shows an STI cryocooler that is currently in production.

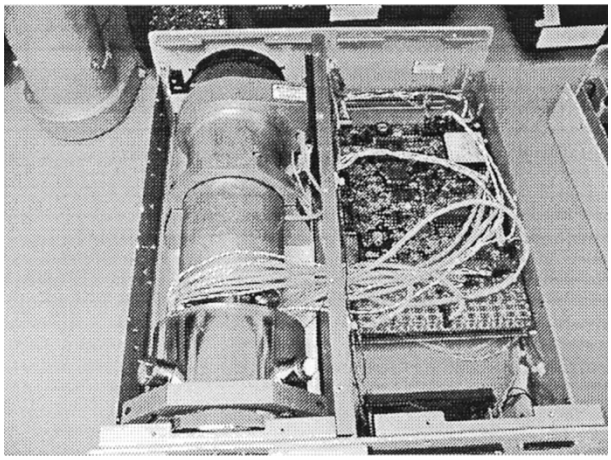

Fig. 1. STI's 19-in rack mount HTS filter system (cooler and Dewar are on the left-hand side, control and power supply electronics on the right-hand side).

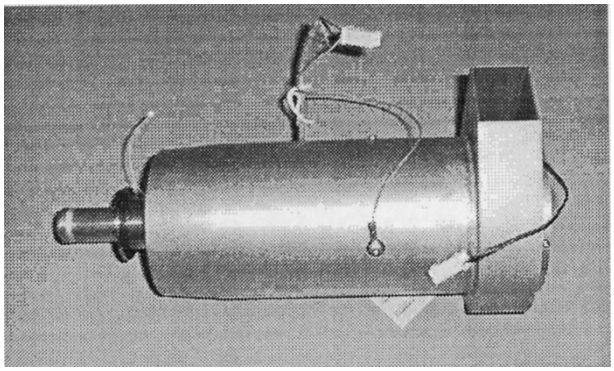

Fig. 2. Cryocooler currently in production at STI.

TABLE I
PERFORMANCE SUMMARY

ITEM	PERFORMANCE
Heat lift at 77K and heat reject of 33°C	4.5 watt minimum
Power input to cryocooler	100 watt maximum
Mass of cooler as shown in Figure 1	4.8 lbs max.
Life/reliability	Greater then 5 years
Size	4.0 in dia. x 13.5 in length
Heat of compression heat reject method	Forced air

A. Performance Summary

The summary tabulated in Table I is based on actual performance data.

B. Description of Critical Technology Components

1) Linear Motor for Free Piston Stirling Cooler: Over the last 20 years, many configurations of linear motor driven compressors for Stirling cryocoolers have been analyzed, developed, and tested. These included moving iron, moving coil, and moving magnets. More detailed information on the

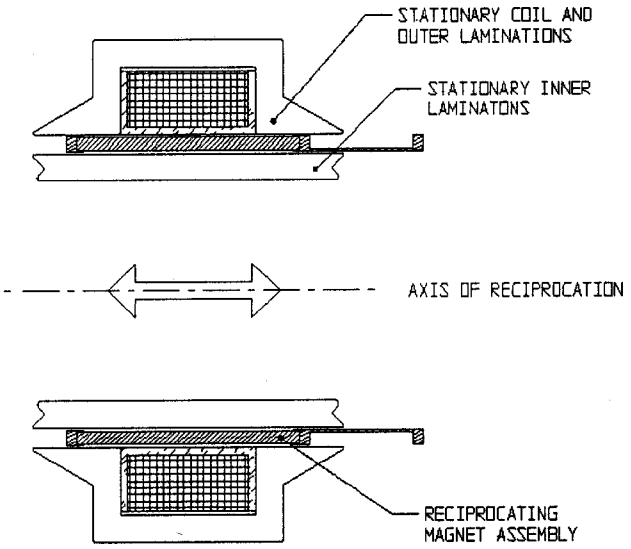

Fig. 3. Cooler magnet cross section.

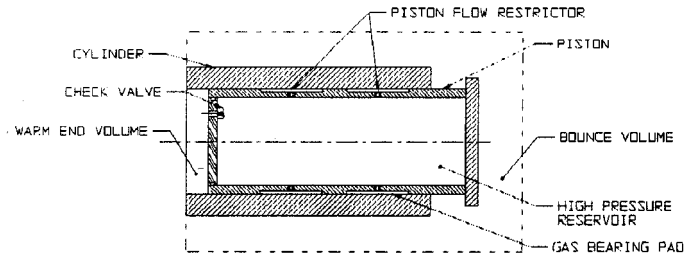

Fig. 4. Cross section on cooler piston.

advantages and disadvantages of each linear motor has been discussed in several technical papers and text books over 20 years.

2) Moving Magnet: The moving-magnet configuration has been used exclusively for about ten years, in sizes ranging from a few watts to 10 000 W. This particular design concept is especially suited for the "free piston Stirling cryocooler" that utilizes a gas bearing to float the compressor piston with the working helium gas.

The arrangement of the stationary coil, stationary outer laminations, stationary inner laminations, and the reciprocating moving magnet, shown in Fig. 3, is utilized in this cryocooler. All of the difficulties associated with other moving magnet configurations and with other types of linear motors are either eliminated or eased to the point where they can be overcome.

3) Motor Efficiency: For this application, minimum system power is an objective. Motors similar in design to the one that will be used in this application have shown efficiencies of 92% with verification by dynamometer tests. Greater efficiencies can be attained at higher cost. The efficiency remains almost constant from rated power down to about 25% of rated power. (Fig. 4) The mechanical power output for this motor is 100 W.

4) Other Design Features: No moving magnet configuration will have a decisive advantage when compared to others on a basis of equal frequency, efficiency, demagnetization temperature, magnet energy, and saturation flux density. The primary criteria for this cryocooler, due to the application (Commercial HTS RF filter systems) are: 1) high reliability; 2) greater than five-year life; 3) high efficiency; and 4) low cost.

For a free piston Stirling cryocooler that utilizes a gas bearing compressor, there are less obvious factors that can cause serious practical problems. These are: 1) magnetostatically generated axial forces; 2) torque; and 3) side forces, which exist in some other linear motor configurations, but not in the type to be used in this application.

The efficiency of the motor to be used in this application is not degraded by strong ac fringing fields, which exist in some other linear motor types and can induce serious eddy current loss in surrounding structure. The system electromechanical control/drive electronics simulation analyses are greatly simplified due to the linearity of the motor. After consideration of all the required factors, analysis, development, and tests, it is the motor designed for this application that makes this cryocooler operate reliably and efficiently.

C. Gas Bearing

The cryocooler utilizes a gas-bearing scheme to ensure long cooler life. The gas bearing eliminates contact between the compressor piston and the compressor cylinder, hence, eliminating friction, except during startup. The piston essentially floats on a thin layer of helium gas, which is the same gas used as the working fluid for the thermodynamic processes within the cooler. A cross section of the piston–gas-bearing–cylinder assembly is shown below in Fig. 4.

During cooler operation, the high-pressure reservoir is kept at a relatively constant and high pressure by the action of the check valve. During the portion of the cycle where the working pressure in the warm end of the cooler is higher than the pressure of the high-pressure reservoir, helium flows from the warm end into the reservoir and "recharges" it ($<$5% of the compressed gas is used for the gas bearing). During the time when the warm end pressure is lower than the reservoir pressure, the check valve closes, preventing helium from escaping from the reservoir. During the entire cycle, helium is flowing from the reservoir through the piston flow restrictors and into the bounce volume.

V. Dewars

Given that cooling is necessary for the HTS, there is a need to package everything in a vacuum insulated environment in order to maintain the operating temperature of the HTS and cryogenic circuitry. The cryopackaging technology employed by STI is adapted primarily from the infrared detector industry, which has been in existence for 35+ years and is now itself heading into the commercial arena. The techniques utilized in packaging an infrared detector or an HTS circuit are very similar until one gets to the functional specifics of the devices in question.

STI has been designing, developing, and producing its own vacuum packaging and necessary subcomponents (such as LNA's, RF cables, and feedthru's) for the last eight years. This has been necessary due to the uniqueness of HTS devices and to ensure total system compatibility and functionality to stay competitive in the wireless telecommunications industry.

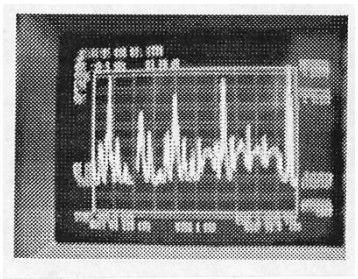

(a)

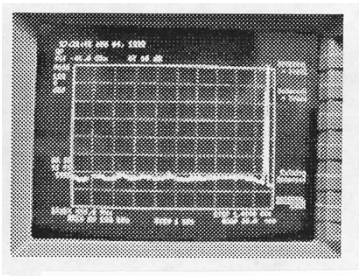

(b)

Fig. 5. Example of interference rejection. (a) Without HTS filtering (b) With HTS filtering.

Vacuum packaging provides the thermal/vacuum insulation required in order to eliminate two of the principal modes of heat transfer: gaseous conduction and convection. The other modes of heat transfer, i.e., radiation and solid structural conduction, are minimized by the careful design and material choices of all of the components going into the Dewar. The longevity of the vacuum package is also of great importance and is integral with thermal design aspects of the Dewar. Bulk materials, platings, adhesives, etc. "outgas" over time in a vacuum environment, thereby decreasing the level of vacuum insulation. Due to this, the processing and handling of the materials chosen become significant. STI's expertise in this technology has yielded Dewars that are still operational in excess of five years.

VI. CryoLNA's

Since the HTS filters need to be cooled, one can gain great advantage by placing as many components as possible in the Dewar. By placing the first-stage LNA in the Dewar, one gains a great advantage in noise temperature. A very good conventional C-band SATCOM LNA has a noise temperature of about 30 K, but by placing a cryoLNA (i.e., an LNA designed to operate at 77 K) in the Dewar with the filter, the noise temperature of the device is only about 10 K. These two elements together provide a very high-performance front end.

Example 1

An example of the advantage of this combination is seen in Fig. 5. The LNA used is a conventional device built by MITEQ, Hauppauge, NY, and modified for use at 77 K in a vacuum environment. The amplifier has a gain of 28 dB and an input return loss of 20 dB. Power consumption is about 400 mW. The noise temperature of this amplifier is 8 K. All these amplifier characteristics are measured at 77 K. The equivalent block diagram is seen in Fig. 6. Fig. 5(a) shows a spectrum analyzer display of all the signals after the first-stage LNA without a filter. Fig. 5(b) shows what the spectrum with the HTS filter included. This clearly shows the improvement in the system by interference rejection. This is where the benefits of superconductors can be realized. By using HTS, small nearly lossless filters can be built, which provide very good selectivity with minimal increase in system noise temperature. The filter used above was designed and built to cover one transponder band with a bandwidth of 37 MHz at a center frequency of about 3.5 GHz. The filter is an eighth-order 0.01-dB equal-ripple Chebyshev design. This filter was fabricated on a 16 mm $\times$ 34 mm MgO substrate that was 0.5-mm thick. An S-parameter plot of the performance of the filter is shown in Fig. 7 with the corresponding physical realization seen in Fig. 8. The design techniques used to synthesize this filter differed significantly from previously published design methodology [2]. From this physical layout, one

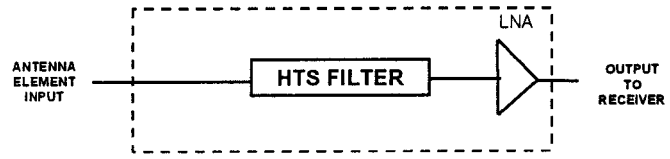

Fig. 6. Block diagram of filter/cryoLNA in Dewar.

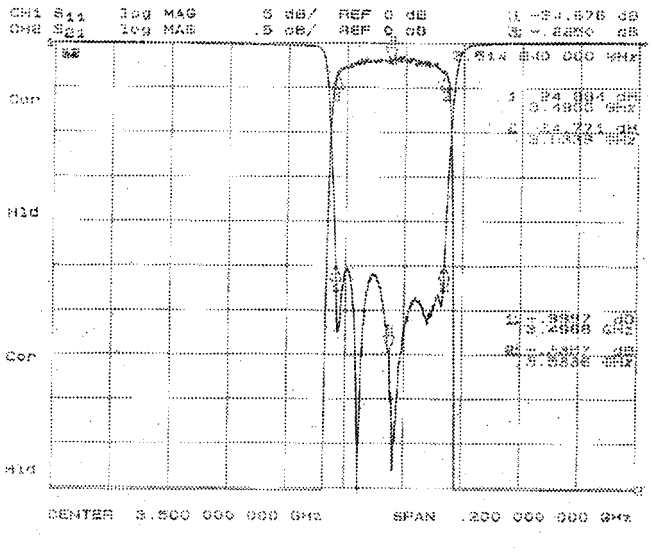

Fig. 7. Plot of S-parameters of eighth-order filter.

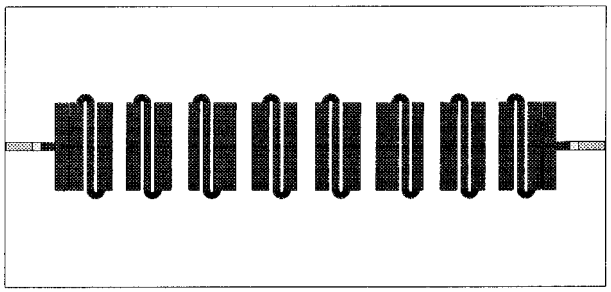

Fig. 8. Physical layout of eighth-order filter.

can see that the resonator used was a half-wave structure with two bends. Instead of optimizing this filter in the lumped domain, as done in other work, the filter performance was optimized directly in the distributed domain. This design approach was chosen because this structure closely resembles a half-resonator and, therefore, becomes practical to optimize directly as distributed elements. The measured passband insertion loss of this filter was about then 0.2 dB and had a return loss of approximately 25 dB. As this filter loss is a cold loss (at 77 K), the added noise temperature due to the filter is only 3.6 K. Thus, the advantage of HTS filters is in providing very high selectivity with only minimal increase in noise temperature that is not normally achievable with normal ambient temperature filters.

Example 2

Another area where HTS filters can provide a huge advantage is jamming resistance. To illustrate the benefits HTS brings to a military SATCOM system, let us examine the effects a single large RF signal has on the performance of a system. As stated earlier, the first component in the RF chain after the antenna in a conventional SATCOM system is usually an amplifier. A single large RF signal could have the effect of degrading the sensitivity of the receiver by saturating the first-stage amplifier. Also, two large RF signals incident on the amplifier that may not be of a level to saturate the amplifier, but also could produce a large number of spurious signals in band due to intermodulation distortion. The best way to deal with this problem is to put a very narrow filter before the amplifier, matched to the bandwidth of the signal of interest. To demonstrate this, STI built an 8-MHz bandwidth bandpass filter centered at about 3.7 GHz. This filter was a sixth-order equal-ripple Chebyshev design patterned on a 16 mm $\times$ 34 mm $\times$ 0.5 mm MgO substrate. The physical structure can be seen in Fig. 9. In order to achieve the low loss to make this narrow passband filter practical in a system, the individual resonator unloaded Q's were approximately 30 000 at 4 GHz. The filter characteristics are optimized to provide the needed protection to the amplifier while passing the signals of interest.

The narrow-band fixed-frequency filter described above would only be effective when the jamming signal is not in the frequency band of interest. If the jammer is frequency agile and able to move into the frequency band of interest, the receiver likewise has to frequency hop to avoid in-band jammer interference. If the jammer lands on the exact frequency you are receiving, the front-end filtering will not help. To demonstrate this concept, STI built a complete cryogenic system that included an LNA, two 8-MHz-wide filters, with center frequencies separated by 16 MHz, and switch networks to switch between the two filters. A block diagram of this system is shown in Fig. 10.

A single-pole double-throw (SPDT) switch is used on both the input and output of the filters to achieve frequency agility. This concept is easily extendable to many more filters simply by nesting the switches or building an SPNT switch, where N is the number of switch positions. The switching networks are located in the Dewar and, thus, gain two advantages by operating the switches at 77 K instead of normal temperatures around 290 K. First, the loss of the switches is a function of temperature. As

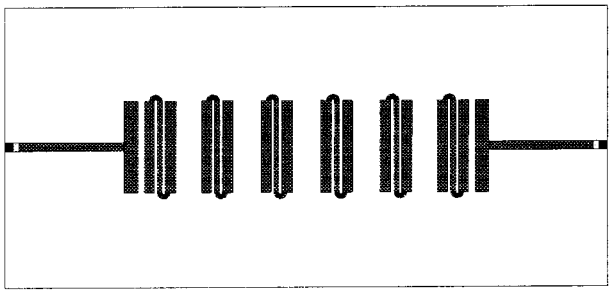

Fig. 9. Physical layout of sixth-order filter.

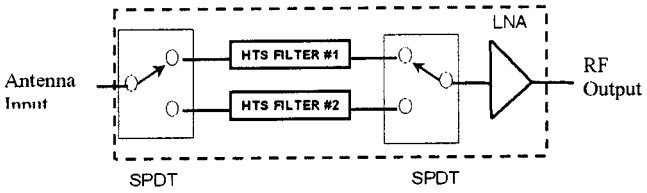

Fig. 10. Block diagram of two-channel switched filter front end.

the temperature decreases, so does the loss. Another important, yet subtle feature is the improvement in noise figure. At room temperature (290 K), the noise figure of a component is equal to the resistive loss of that component. For example, a 3-dB pad at 290 K would have a noise figure of 3 dB and a noise temperature of 290 K. However, at 77 K, this no longer holds true as the noise temperature is reduced to 77 K. Due to the definition of noise figure, the noise figure of a 3-dB pad at 77 K is 1.02 dB. Due to this difference in using noise figure, it is less confusing to talk about noise contributions in terms of noise temperature. An SPDT RF switch was designed to operate at 3.70–3.74 GHz, with minimum insertion loss and return loss, maximum isolation, and to consume as little power as possible, for use in a two-channel SATCOM switchable filter unit. The circuit was to fit within an area of 0.4 in $\times$ 1.0 in. It was to receive a TTL signal to switch between two RF paths within 125 μs.

VII. Monolithic-Microwave Integrated-Circuit Switch

GaAs monolithic-microwave integrated-circuit (MMIC) switches were used for the switching module. The reason for using GaAs MMIC's is their small size and temperature dependency of their insertion loss. An SPDT switch can be mounted, along with necessary biasing circuitry, on a substrate that would easily fit the form of the existing microenclosure (one substrate at the input and another at the output). Resistive losses of GaAs decreases as temperature decreases (approximate loss change of 0.0025 dB/°C, from -55 °C to $+85$ °C as specified for M/A-COM, Los Angeles, CA, GaAs MMIC switches).

After careful consideration, the choice for the MMIC switch to be used was narrowed down to two. The first was a low —loss reflective switch manufactured by M/A-COM (part number MASW6010G). The other was a high-isolation terminated (nonreflective) switch with slightly higher loss than that of the

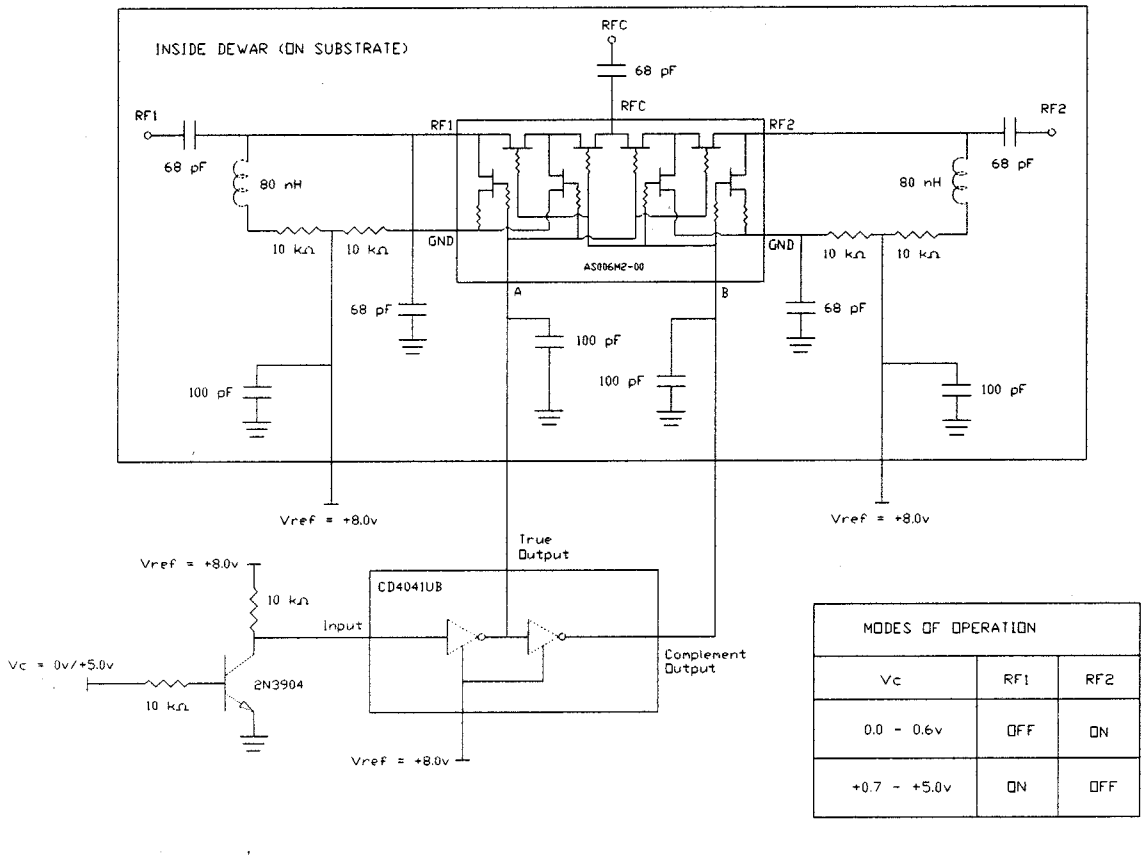

Fig. 11. Schematic diagram of switch module with bias/control circuitry.

M/A-COM part. This was manufactured by Alpha Semiconductor, Pleasanton, CA (part number AS006M2-00). The two switches were available in die form (i.e., not packaged). Both were SPDT dual-input control switches. The MASW6010G switch had the lowest insertion loss of any off-the-shelf MMIC switch operating at around 4 GHz. It was specified at 0.5-dB typical insertion loss at 4 GHz, and 0.6 and 1.4 dB maximum at 2.0 and 6.0 GHz, respectively. Its input/output isolation performance specification was 38 and 22 dB minimum at 2.0 and 6.0 GHz, respectively. The AS006M2-00 was specified at 1.4-dB maximum insertion loss (typically 1.1 dB) and 45-dB minimum isolation at 4 GHz. All these specifications were for 25 °C.

A. Initial Testing

Since insertion loss directly affects noise figure, it was considered the most important specification, emphasis was placed on the M/A-COM switch. The MASW6010G switch was first tested on a substrate with 50-Ω thru lines at its input and output. It was mounted on a wraparound ribbon to ground and its ground pads wire bonded to the gold ribbon. This approach resulted in low input/output isolation at approximately 10–15 dB. The parameters that need to be considered in this degradation of isolation are the inductance of the wire bonds and the ribbon between the ground pads and the actual ground plane of the test circuit.

To improve isolation, the switch had to be mounted as close to the ground plane as possible. The simplest way to achieve this in a test circuit was to mount the switch directly on the package, which acted as the ground plane of the circuit. Two thru-line substrates were mounted on the package at the input/output of the switch. In this configuration, the top of the switch and the thru lines were almost at the same level, reducing the necessary input/output bond wires. The ground pads of the switch were directly wire bonded to the package. The resulting isolation was approximately 22 dB.

The actual switch insertion loss was found by measuring the test circuit with the switch and with the switch replaced by gold ribbon. Taking the difference between the two measured results gives the insertion loss of the switch. Typically, the insertion loss of the switch was 0.8 dB at room temperature and 0.5 dB at 77 K.

Input switch isolation between the common port and port 1 was measured with a filter at port 2 terminated with a short. The result was 18 dB at 3.7 GHz, approximately 4 dB lower than when the switch was measured with a matched load. The input switch isolation degraded because the switch did not have internal terminations and was designed for 50-Ω external termination for optimum performance. The filter had a 50-Ω input impedance only if the output was terminated with 50 Ω. In this case, the output of the filter saw a short/open because the output switch was “off,” and in-turn did not provide the input switch a good match. The output switch also has the same problem, thus, its isolation would also be 18 dB. The total isolation of the system with both input and output switches and filters would only be 36 dB.

To eliminate this problem, a terminated switch would have to be used since load impedance does not affect isolation in terminated switches. The decision was made to utilize the AS00M2-00 switch. Nearly 0.3 dB of insertion loss per switch was sacrificed to gain the isolation needed.

B. Switch Module

The switch module contained the MMIC switch, bias circuitry, and interconnects. The interconnects between the switch and filters were coplanar-waveguide transmission lines with a ground plane (CPWG). Channelization of the transmission lines aided in isolating the RF paths. The top layer of the substrate was grounded through via holes to the ground plane, with the exception of the center conductor of the CPWG transmission lines and the mounting pad for the switch. The backside of the switch was isolated from ground because of the biasing scheme, which will be discussed later. Chip capacitors (68 pF) were used as dc blocks along the RF paths. They were mounted directly on the CPWG center conductor and bonded in series with the line.

C. Biasing/Switch Controller Circuitry

Part of the switch control and bias circuitry resided on the substrate (inside the Dewar), with the rest outside the Dewar. The control voltage to be supplied for switching the circuit was TTL based. The simplest way to implement this control was to use the CMOS true-complement buffer chip CD4041UB to provide the control voltages. The TTL control signal had to be converted to the proper voltage for switching the MMIC. This was done using a 2N3904 n-p-n transistor. The new control voltage was input into the CD4041UB chip, which provided simultaneous zero and positive outputs to the MMIC switch. Since the MMIC switch needed a negative voltage for switching, the dc ground of the switch had to be floated to positive voltage. Now the MMIC switched from $+V$ to zero, instead of zero to $-V$. To float dc ground and keep RF ground, chip capacitors (68 pF) were used between the ground pads of the MMIC and the top layer ground plane. The reference voltage for floating dc ground was applied to the RF ports (ports 1 and 2 or drain terminals of the FET's of the switch) and the MMIC ground pads (source terminals of the FET's of the switch) because both the source and drain had to be floated. Resistors between the input voltage terminals and the MMIC were used for protection, as well as isolation between ports 1 and 2. Air core inductors (80 nH) were used for added isolation between the RF ports, and to isolate the dc reference voltage from the RF path. Chip capacitors were used as RF bypass at the dc inputs to keep high-frequency noise out of the circuit. A schematic representation is seen in Fig. 11.

D. Final Data

The insertion loss of the switch module utilizing the AS006M2-00 chip was approximately 1.0 dB at 77 K, with better than 1.3 : 1 input/output VSWR in the band of interest (3.70–3.74 GHz). Input/output isolation provided by the module was greater than 30 dB in the band of interest. The isolation between channel one and channel two of the switch module was also greater than 30 dB in the band of interest.

TABLE II
COMPARISON OF TWO ANTENNA TYPES

	2.4m Antenna	Dual 1m Antenna
Aperture Size	4.52 m^2	1.57 m^2
Anti-Jam	0 dB	> + 14 dB
Gain	37 dB	32 dB
Beamwidth	2.3 degrees	2.3 degrees

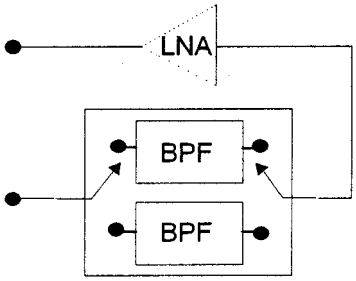

(a)

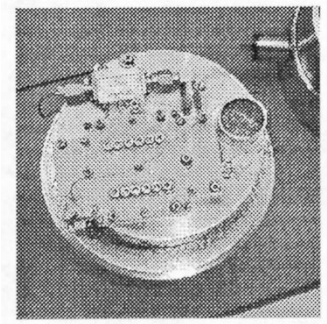

(b)

Fig. 12. SATCOM microenclosure. (a) Block Diagram. (b) Physical Layout.

Switching time of the module was not measured, although it was predicted to be much less than 1 μs.

Now with the filters, cryoLNA, and MMIC switches ready, we move onto the demonstration.

VIII. DEMONSTRATIONS

The demonstration consisted of two parts. In the first part, we compared the performance of a 2.4-m dish with a conventional LNA to that of SRI's two 1-m dishes with a cryogenic LNA. To achieve spatial filtering equivalent to the larger dish, SRI's antenna array placed nulls on the next nearest neighbor satellites. We showed that the much smaller two-dish array with the cryogenic LNA has equivalent performance to the 2.4-m dish mated with a convention LNA, as shown in Table II. The cost of the cryogenic LNA is more than offset by the cost saving and convenience in not having such a large dish, which together with the smaller size, gives the advantage of producing a much more portable system. This would be a great advantage in a modern tactical battlefield situation where portability is a primary consideration.

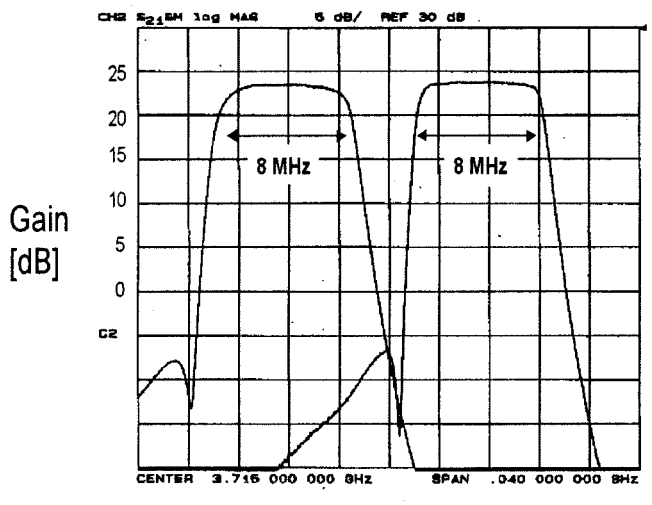

Fig. 13. Plot of the two passband states of the two-channel switched-filter front end.

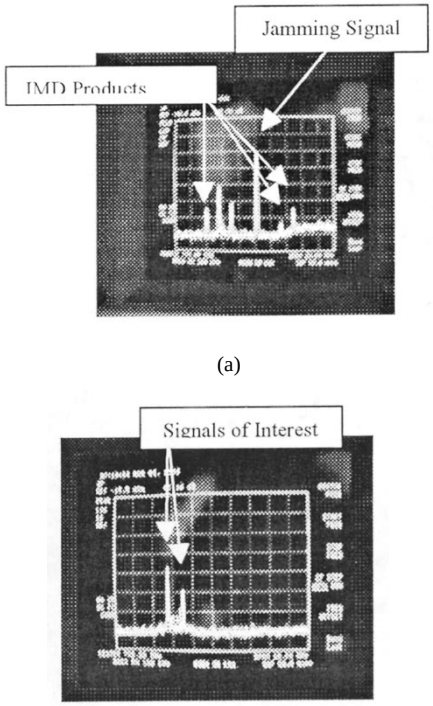

(a)

(b)

Fig. 14. Example of jamming resistance. (a) Jammed—no HTS filter. (b) Jammed—with HTS filter.

The second part of the demonstration consisted of showing the frequency agility possible with the use of HTS filters. STI had two systems at the demonstration. One Dewar had two filters in it, as shown in Fig. 12. The performance of the unit is shown in Fig. 13. The other Dewar had a single filter in one path and a through transmission line in the other path. To show the antijam capability, the Dewar with one filter and through line was selected so that the effect of jamming could be shown. In the demonstration, a probe was placed in the antenna array near field pattern to inject a television signal. The frequency of the television signal was such that it was in the center of the passband of the filter. The system was set in the thru-line configuration, then a single large jamming signal was injected into the antennas through the same probe as the signal of interest. This resulted in the spectrum seem in Fig. 14(a). The state of the system was switched to the filtered path and the resulting spectrum is seen in Fig. 14(b). One can see that with the jammer, the desired signal strength is reduced by about 4 dB due to the degradation of the amplifier and a resultant decrease in the signal-to-noise ratio for the required signal. There are also intermodulation products due to the mixing of the jamming signal and television signals. When the filter is in the system, the amplitude of the desired signal is larger, and there are no other signals. For ease of the demonstration, these spectrum plots were taken down the RF chain at the first IF. One can see by extension that, by using multiple filters before the LNA (e.g., the two-channel unit shown in Fig. 11), the system can improve resistance to a frequency agile jammer if both the transmission frequency and filter selection is done synchronously.

IX. Conclusion

As explained previously, with SRI's small antenna array and STI's cryogenic filter and amplifier, a very high-performance frequency-agile front end can be built. This can result in a jam-resistant SATCOM system for tactical battlefield applications. While STI's demonstration only consisted of two filters, the architecture can easily be extended to include many more filters by increasing the switch to have more connections. The introduction of cryogenics into a system, including more of the RF chain in the Dewar, results in greater benefit to the system.

Acknowledgment

The authors would like to thanks D. Ellis, SRI International, Menlo Park, CA, and E. Fernandes, SRI International, Menlo Park, CA, for all their assistance.

References

[1] T. Dahm and D. J. Scalapino, "Theory of intermodulation in a superconducting microstrip resonator," *J. Appl. Phys.*, vol. 81, p. 2002, 1997.

[2] G. L. Hey-Shipton, "Efficient computer design of compact planar bandpass filters using electrically short coupled lines," in *1999 IEEE MTT-S Int. Microwave Symp. Dig.*.

Edward R. Soares (M'98) received the B.S. degree in physics from the University of California at Santa Barbara, in 1993.

In 1989, he joined Superconductor Technologies Inc., Santa Barbara, CA, as an Intern, and began his full-time employment upon graduation. His primary interest is in filter design.

Jeffery D. Fuller (M'86) received the B.S. in engineering from the University of California at Los Angeles, and the M.S.E.E. degree from the Naval Postgraduate School, Monterey, CA.

Upon completion of military service, he joined Superconductor Technologies Inc., Santa Barbara, CA, where he has been involved with the design of superconducting filters and LNA's.

Phil J. Marozick received the B.S. degree in Aerospace Engineering from the U.S. Air Force Academy, Colorado Springs, CO.

He has performed work for the U.S. Air Force, Gyrex Corporation, Scientific Research Laboratories, DSI Micro, and Superconductor Technologies, Santa Barbara, CA.

Robby L. Alvarez received the B.S. degree in electrical and computer engineering from the University of California at Santa Barbara, in 1995.

He is currently an Engineer at Superconductor Technologies Inc., Santa Barbara, CA. His current focus is on the design and development of next-generation superconducting filters for the wireless industry.